Transactions of the Materials Research Society of Japan 26 [3] 1041-1044 (2001)

Properties of $LiNbO_3$ films deposited by pulsed laser deposition under various oxygen ambients

K. Matsubara, P. Fons, A. Yamada, K. Iwata, and S. Niki
Electrotechnical Laboratory, Umezono 1-1-4, Tsukuba, Ibaraki 305-8568 JAPAN
Fax: 81-298-61-5627, e-mail: koji@etl.go.jp

The crystallinity and composition of $LiNbO_3$ films deposited by pulsed laser deposition under various oxygen ambients were compared. $LiNbO_3$ films were deposited 1) in an O_2 atmosphere, which is normally used to deposit oxide films, and 2) with oxygen radical irradiation onto the growing surface. The film deposited in a molecular O_2 atmosphere under low oxygen partial pressure ($\sim 10^{-5}$ Torr) displayed a significant deficit of lithium and oxygen, and its chemical composition did not correspond to $LiNbO_3$. The shortage of lithium and oxygen was still observed in the films deposited in molecular O_2 gas with an oxygen partial pressure of 7.0 x 10^{-2} Torr. Though the oxygen partial pressure was as low as 10^{-5} Torr in the films deposited with the oxygen radical irradiation, good crystallinity and film compoition same as the target were achieved.
Key words: pulsed laser deposition, $LiNbO_3$, epitaxial films

1 INTRODUCTION

$LiNbO_3$ is widely used for surface acoustic wave (SAW) filters for mobile phones and TVs, pyroelectric sensors, and a variety of optical devices such as optical waveguide switches, modulators, and nonlinear wavelength converters. Such optical waveguide devices are normally made by means of impurity diffusion into bulk $LiNbO_3$ crystals, though the optical confinement and interface sharpness of such devices need improvement. With a sharp change of refractive index at the interface, light energy is strongly confined to the waveguide region resulting in enhanced device performance. For example, the conversion efficiency of second harmonic generation devices could be greatly enhanced by this effect. Heteroepitaxial structure of a $LiNbO_3$ layer on substrates whose refractive index is lower than $LiNbO_3$ would be a promising candidate for such a discontinuous change of refractive index and high performance optical waveguide devices.

There have been numerous reports on producing $LiNbO_3$ thin films; sputtering [1, 2], liquid phase epitaxy (LPE) [3, 4], molecular beam epitaxy (MBE) [5], wet-processes [6], metalorganic chemical vapor deposition (MOCVD) [7], and pulsed laser deposition (PLD) [8, 9, 10]. As a consequence of its great success in the growth of high temperature superconducting materials [11], PLD has been shown to be a promising method to grow oxide compounds including $LiNbO_3$. Compared to other techniques, PLD has an advantage of an easy transfer of target composition to the growing film. However, oxygen atoms tend to desorb during PLD in the growth of oxide compounds. To compensate for the oxygen deficiency, O_2 molecular gas is commonly used as an ambient gas [9]. O_3 gas has also been used to increase oxygen reactivity [10]. We have used an r.f. radical source to provide oxygen radicals which have higher reactivity than O_2 molecules, and obtained high quality $LiNbO_3$ epitaxial films on c-sapphire substrates [12]. In this work, we compare the crystallinity and chemical composition of films deposited with different oxygen sources: O_2 molecular gas and oxygen radicals.

2 EXPERIMENTS

$LiNbO_3$ films were grown by a pulsed laser deposition system. The growth chamber was evacuated by a turbo molecular pump down to a base pressure of 10^{-9} Torr. A growth chamber equipped with load-lock one enabled to change samples or targets without breaking vacuum. A KrF excimer laser beam (wavelength: 248 nm; pulse width: 30 ns; fluence: ~ 1 J/cm^2; repetition rate; 10 Hz) was loosely focused by a quartz lens on the rotating target. The incident angle of the laser beam was about 40° from the target normal. The ablation target was a $LiNbO_3$ single crystal grown from a congruent melt whose Li/Nb ratio was nearly unity. The target was rotated during growth to avoid pitting of the target surface. A single side polished sapphire (0 0 0 1) substrate was placed opposite to the target, after sequential cleaning in ultrasonic baths of acetone and ethanol and boiling in ethanol. The substrate was fixed on a substrate holder made of Inconel with Inconel clips and heated with a lamp heater from the back side. Thermal cleaning of the substrate was done at 600°C in the growth chamber just before growth. The films were, subsequently, grown at 600°C. The substrate temperature was monitored by an infrared radiation thermometer. The substrate was rotated during growth to improve film uniformity. The distance between the target

and the substrate was about 60 mm. Oxygen was supplied in two different forms: molecular O_2 gas (purity: 99.9995 %) introduced through a variable leak valve and oxygen radicals produced by an r.f. radical cell equipped with an ion trap. The flow rate of O_2 gas was controlled by a mass flow controller (MFC). The r.f. radical cell was fitted with an optical fiber so that optical emissions from the plasma could be observed in real time. After deposition, oxygen supply was immediately stop and the temperature of the substrate was gradually decreased ($\sim$1°C/min).

The crystallinity of deposited films was examined using a X-ray diffractometer (XRD) with a Cu $K\alpha$ rotating anode generator. X-ray photoelectron spectroscopy (XPS) using a Mg $K\alpha$ (1253.6 eV) radiation was carried out to determine the chemical composition of the films. As XPS was performed after the samples were removed from the growth chamber into air, the surface of the film was sputtered by Ar ion in the XPS chamber before measurements to eliminate surface contamination. To exclude selective sputtering effects by the ion bombardment, a bulk $LiNbO_3$ crystal was also sputtered to provide a standard.

3 RESULTS AND DISCUSSIONS

Films prepared under three different oxygen supply conditions were listed in Table I. Films O_2-1 and O_2-2 were deposited in the O_2 ambient. The oxygen partial pressure P_{oxygen} during deposition of Film O_2-1 was 7.0 x 10^{-2} Torr, which is the same order as generally used to deposit oxide compound films by PLD [13]. The P_{oxygen} value for Film O_2-2 was 1.3 x 10^{-5} Torr. Film R was deposited with oxygen radical irradiation. The O_2 flow rate and applied r.f. power were 0.3 sccm and 300 W, respectively. Pressure during deposition was 1.3 x 10^{-5} Torr. The plasma emission spectrum had a dominant peak at λ = 777 nm, corresponding to the (3s $^5S^\circ$ - 3p ^5P) transition of neutral oxygen atoms[14]. A peak one eighth the intensity of the 777 nm peak was observed at 845 nm which corresponds to the (3s $^3S^\circ$ - 3p ^3P) transition.

Table I: Oxygen supply conditions

Name of film	Oxygen ambient
O_2-1	O_2: 7.0 x 10^{-2} Torr
O_2-2	O_2: 1.3 x 10^{-5} Torr
R	Radical: 1.3 x 10^{-5} Torr

XRD patterns along the surface normal (2θ-ω scans) are shown in Fig.1; from 2θ = 5° to 85°. The sapphire (0 0 0 6) peak is marked with the symbol "•". Peaks marked with a diamond symbol came from the thermal treated substrate or the stainless

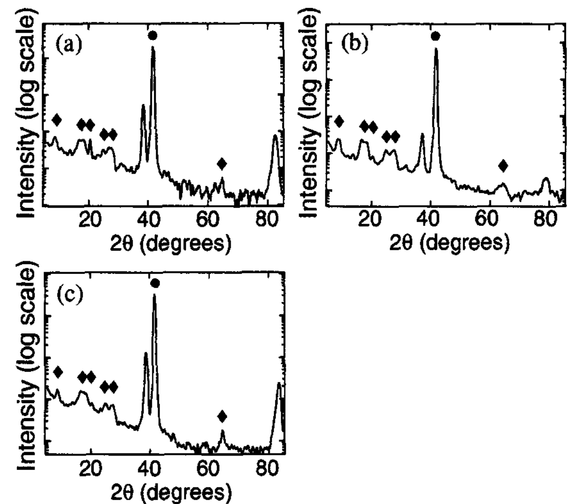

Figure 1: XRD patterns along the surface normal. (a) Film O_2-1, (b) Film O_2-2, (c) Film R. The "•" symbol denotes the sapphire (0 0 0 6) reflection; Peaks marked with the diamond symbols are due to the thermally treated substrate or the stainless steel holder.

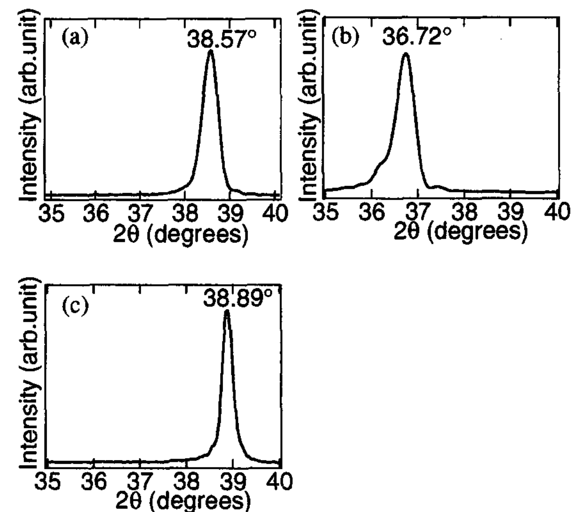

Figure 2: 2θ-ω scans in vicinity of $LiNbO_3$ (0 0 0 6) peak. (a) Film O_2-1, (b) Film O_2-2, (c) Film R.

steel sample holder of XRD system. All films displayed a peak around 2θ = 36°$\sim$39°. Films O_2-1 and R displayed an additional peak around 2θ = 82° $\sim$ 83°. This peak corresponds to the $LiNbO_3$ (0 0 0 12) reflection. These results show that c-axis oriented films were grown.

Figure 2 shows 2θ-ω scans in the vicinity of $LiNbO_3$ (0 0 0 6) peak; the peak position for bulk $LiNbO_3$ crystal is 38.94°. The peak position of Film O_2-2 is $\sim$ 2° smaller than that of bulk crystal. In $LiNbO_3$ (1 0 $\bar{1}$ 4) pole figure measurements, no peak was observed for this film as shown in Fig.3 (b). This implies that a material other than $LiNbO_3$ was produced. Though the oxygen pressure was as low

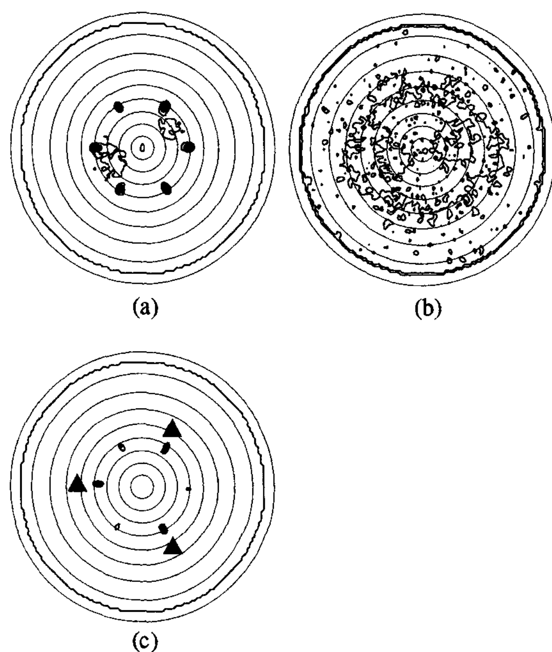

Figure 3: $LiNbO_3$ (1 0 $\bar{1}$ 4) pole figures. (a) Film O_2-1, (b) Film O_2-2, (c) Film R.

as 1.3×10^{-5} Torr, the peak position for Film R was 38.89°. From this value, the calculated *c*-axis lattice constant of the film is 0.1 % larger than that of bulk $LiNbO_3$. The peak position of Film O_2-1, 38.57°, implies that the calculated *c*-axis lattice constant is 0.9 % longer than bulk crystal. The peak width was narrower for Film R than for Film O_2-1.

The results of $LiNbO_3$ (1 0 $\bar{1}$ 4) pole figure measurements are shown in Fig.3. Films O_2-1 and R displayed six-fold symmetry while $LiNbO_3$ bulk crystal has three-fold symmetry as it belongs to 3m (C_{3v}) point group. This implies the presence of 60° in-plane rotational twins in both films. While the peak intensities for Film O_2-1 were similar for all of the six peaks, those for Film R could be classified into two groups; the three peaks marked with triangle symbols were approximately ten times more intense than the other three peaks. These dominant peaks demonstrate that the *a*-axis of Film R tends to align with the *a*-axis of sapphire substrate. The $LiNbO_3$ (1 0 $\bar{1}$ 4) peaks were also narrower for the film R than for Film O_2-1. These 2θ-ω scans and pole figure measurements show that crystallinity of the film R was better than Film O_2-1.

Figure 4 show the Li/Nb and O/Nb ratios calculated from XPS analysis. In Film O_2-2, no lithium peak was observed and the O/Nb ratio was 2.5 or less. This result also implies that Film O_2-2 was not $LiNbO_3$ but NbOx (x $\sim$ 2.4). Film O_2-1 still displayed a significant deficiency of lithium and oxygen while Li/Nb and O/Nb ratios of Film R were as same as the bulk crystal*. We attribute this advan-

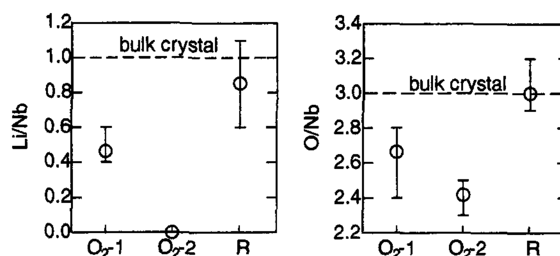

Figure 4: Li/Nb and O/Nb ratios calculated from XPS results. Dashed lines show the values for a bulk reference crystal.

tage of our system to high reactivity of oxygen radicals. Due to its high reactivity, 1) species ablated from the target were effectively oxidized and fixed on the substrate surface, preventing from desorption; 2) deposition under lower pressure was possible, providing long mean-free path of the species, especially for light elements such as lithium. In sputtering or PLD of $LiNbO_3$ films, this type of Li_2O deficiency is typically found. To compensate this, a Li-rich target is usually employed to produce oxygen stoichiometric $LiNbO_3$ films by conventional PLD [13]. Li-rich ceramic targets are produced from a sintered mixture of Nb_2O_5 and Li_2O or Li_2CO_3. However it is hard to obtain compound oxides or salts of alkali metals (such as Li_2O and Li_2CO_3) of high purity; e.g. the purest Li_2CO_3 commercially available is only 4N. Using oxygen radical source, a Li/Nb ratio of nearly unity was obtained from the conguruent $LiNbO_3$ crystal target. As single crystal targets are generally purer than ceramic targets, higher purity $LiNbO_3$ crystal film can be anticipated with the use of the radical assisted PLD.

4 CONCLUSIONS

$LiNbO_3$ films were grown with different oxygen supply conditions. XRD and XPS analysis revealed that the use of oxygen radicals was effective to compensate for a shortage of oxygen and lithium in the films. The presence of a different phase due to the lack of lithium and oxygen was observed in the film grown in the typical O_2 ambient with an oxygen partial pressure P_{oxygen} on the order of 10^{-5} Torr. A P_{oxygen} of 7×10^{-2} Torr was necessary to eliminate this phase for a film grown in the molecular O_2 gas ambient. The film grown with the oxygen radical irradiation showed no additional phases, and the stoichiometric composition within the accuracy of the XPS measurement. The crystallinity and composition of the film were also better for the film grown with the oxygen radical irradiation than for that grown in the O_2 ambient.

*The exact Li/Nb ratio of a bulk crystal grown from a congruent melt is 0.946. As we have assumed that the Li/Nb ratio was unity for the bulk $LiNbO_3$ crystal used as a standard to calculate Li/Nb ratio, Li/Nb = 1 is the value for the bulk crystal in Fig.4.

ACKNOWLEDGEMENT

The authors would like to express their thanks to Dr. H. Shibata for his useful discussions.

5 * References

[1] P. R. Meek, L. Holland and P. D. Townsend: Thin Solid Films **141**, 251 (1986).

[2] S. Schwyn, H. W. Lehmann, and R. Widmer: J. Appl. Phys. **72**, 1154 (1992).

[3] T. Kawaguchi, D. Yoon, M. Minakata, Y. Okada, M. Imaeda, and T. Fukuda: J. Cryst. Growth **152**, 87 (1995).

[4] A. Yamada, H. Tamada and M Saitoh: Appl. Phys. Lett. **61**, 2848 (1992).

[5] R. A. Betts and C. W. Pitt: Electron. Lett. **21**, 960 (1985).

[6] K. Nashimoto and M. J. Cima: Mat. Lett. **10**, 348 (1991).

[7] S. Y. Lee and R. S. Feigelson: J. Cryst. Growth **186**, 594 (1998).

[8] S. B. Ogale, R. Nawathey-Dikshit, S. J. Dikshit, and S. M. Kanetkar: J. Appl. Phys. **71**, 5718 (1992).

[9] P. Aubert, G. Garry, R. Bisaro, and J. G. Lopez: Appl. Surf. Sci. **86**, 144 (1995).

[10] Y. Shibata, K. Kaya, K. Akashi, M. Kanai, T. Kawai, and S. Kawai: Appl. Phys. Lett. **61**, 1000 (1992).

[11] P. W. Chan, W. Wu, K. H. Wong, K. Y. Cheung, and T. Jeffrey: J. Phys. D: Appl. Phys. **30**, 957(1997)

[12] K. Matsubara, S. Niki, M. Watanabe, P. Fons, K. Iwata, and A. Yamada: Appl. Phys. A **69**, S679 (1999).

[13] M. Haruna, H. Ishizuki, J. Tsutsumi, Y. Shimaoka, and H. Nishihara, Jpn. J. Appl. Phys. **34**, 6084 (1995).

[14] C. E. Moore, "Table of Spectra of Hydrogen, Carbon, Nitrogen, and Oxygen Atoms and Ions", Ed. by J. W. Gallagher, CRC press, Boca Raton (1989).

(Received December 8, 2000; Accepted January 11, 2001)